6-14-2000

Magnetomechanical performance and mechanical properties of Ni-Mn-Ga ferromagnetic shape memory alloys

Steven J. Murray
Massachusetts Institute of Technology

Samuel M. Allen
Massachusetts Institute of Technology

R. C. O'Handley
Massachusetts Institute of Technology

Thomas A. Lograsso
Iowa State University, lograsso@ameslab.gov

Magnetomechanical performance and mechanical properties of Ni-Mn-Ga ferromagnetic shape memory alloys

Abstract
A Ni-Mn-Ga ferromagnetic shape memory alloy was tested for strain versus applied field and strain versus stress. Field- induced strains up to 6 percent were measured with a hysteresis of about 160 kA/m. The results are compared with the predictions of modeling with a focus on hysteresis. The model is applied to the case in which the magnetic external field and external load are orthogonal to each other. It predicts the magneto-mechanical hysteresis as a function of the yield stress in a twinned martensite. Magnetization versus applied field was measured on a sample that was mechanically constrained in order to understand the magnetization behavior of the sample in the absence of twin motion. These measurements give the magnetic anisotropy and are used to estimate the demagnetization fields. The measured behavior of strain with stress at constant field is approximated by the model.

Disciplines
Metallurgy

http://dx.doi.org/10.1117/12.388253.

Magneto-mechanical performance and mechanical properties of Ni-Mn-Ga ferromagnetic shape memory alloys

S. J. Murray[a], S. M. Allen, R. C. O'Handley
Massachusetts Institute of Technology, Cambridge, MA 02139
[a]Present Address: Mide Technology Company, 57 Rodgers St., Cambridge, MA 02139

and T.A. Lograsso
Ames Laboratory, Ames IA

ABSTRACT

A Ni-Mn-Ga ferromagnetic shape memory alloy was tested for strain versus applied field and strain versus stress. Field-induced strains up to 6% were measured with a hysteresis of about 160 kA/m. The results are compared with the predictions of modeling with a focus on hysteresis. The model is applied to the case in which the magnetic external field and external load are orthogonal to each other. It predicts the magneto-mechanical hysteresis as a function of the yield stress in a twinned martensite. Magnetization versus applied field was measured on a sample that was mechanically constrained in order to understand the magnetization behavior of the sample in the absence of twin motion. These measurements give the magnetic anisotropy and are used to estimate the demagnetization fields. The measured behavior of strain with stress at constant field is approximated by the model.

Keywords: Martensite, Twin Boundaries, Ferromagnetic Shape Memory, Hysteresis

1. INTRODUCTION

Ferromagnetic shape memory alloy's (FSMA) such as Ni-Mn-Ga and Fe-Pd are members of a new class of active materials that exhibit considerably larger strains than conventional active materials. The mechanism of field-induced deformation in an FSMA is the rearrangement of the variant structure of a twinned martensite through the motion of twin boundaries to accommodate the applied field and/or load. The interaction of the variant structure with the applied field occurs because the magnetic moments within each variant are strongly coupled to the crystal structure by magnetocrystalline anisotropy. Unlike magnetostriction, this process does not require rotation of the magnetization from its preferred crystal direction, in fact such rotation reduces the driving force for twin boundary motion in FSMAs. Field-induced twin boundary motion can result in deformation of several percent.

This effect was first observed by Ullakko, et al.[1] who reported a 0.2% reversible strain in Ni-Mn-Ga in 1996. James and Wuttig[2] measured a 0.5% reversible free strain in Fe-Pd and later Tickle et al.[3] reported 1.3% free strain in Ni-Mn-Ga with the application of field on a sample biased to a single variant state by stress-cooling. The theoretical maximum strain is the strain produced by rotating the variant structure 90^o, which is about 6.3% in Ni-Mn-Ga (depending on composition). Experiments involving strain under load have been performed by Murray et al.[5,6] and Tickle et al.[3] James and Wuttig[2], O'Handley[4], and Murray et al.[5,6] have proposed models describing this effect. These models account for magnetic field energy and external stress energy. Further, James and Wuttig[2] include the effect of demagnetization fields micromagnetically, and O'Handley allows for finite magnetocrystalline anisotropy to account for magnetization rotation relative to the crystal axes. The magnetostatic energy is the most difficult to approximate in a simple model due to the non-ellipsoidal shapes of the variants and changes in their shape with applied field. Another element of the material performance that has not yet been explained is the occurrence of hysteresis in the magneto-mechanical response of the material. This

article attempts to explain the hysteresis seen in the magneto-mechanical behavior and describes an approximation for the effects of demagnetization.

A review of the previous modeling work is followed by a description of the effects of hysteresis and the correction for demagnetization fields. Section 3 gives a brief summary of experimental, including experiments to determine the parameters needed to estimate the hysteresis and demagnetization. The results and comparisons with the proposed models are presented in Sections 4 and 5. A discussion of material composition and its relationship to properties is included in the discussion section.

2. MODELING

The present models of performance in FSMAs account for the four energy terms mentioned above (field, stress, magnetostatic and magnetocrystalline anisotropy). These models are most easily understood in the special case in which the magnetic field and external compressive stressare orthogonal to each other and H is parallel to <001>. In the alloy Ni-Mn-Ga, the contraction of the crystal structure along the martensitic c-axis (which is also the magnetic easy axis) causes the alloy to tend to align its short crystal direction with the applied magnetic field. This causes the direction orthogonal to the applied field to elongate, and hence the compressive load in this orthogonal direction works against the magnetic field. The compressive stress would tend to stabilize a variant with a c-axis in the direction of applied stress. If field and stress are orthogonal, transitions between these two variants can be accomplished by the motion of a twin boundary. Neglecting the presence of demagnetization energy, we expect the strain response to have a threshold-type behavior. When the magnetic field energy, M_sH, becomes larger than the mechanical energy, $\sigma\varepsilon_o$, we expect the sample to transform to the variant that is stabilized by the field. The strain of switching between variants with orthogonal c-axis is expressed as ε_o and is related to the tetragonality of the alloy, $\varepsilon_o=1-((c/1.414)/a)$, where c and a are the lattice parameters.

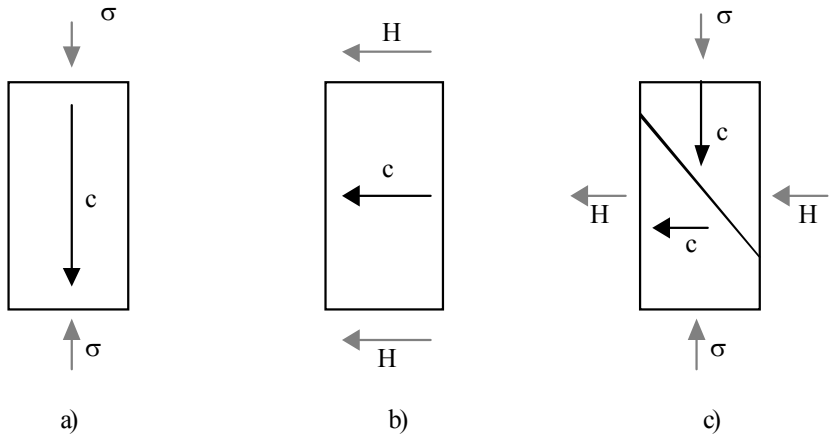

Figure 1. Illustration of the stable states of a sample of FSMA with orthogonal applied field and stress. a) The variant stable under stress b) The variant stable under the applied field c) The twin boundary that relates the two variants.

To further illustrate this process, Figure 1 shows the two stable variant states and the twin boundary relating them. Transformation from the variant in a) to that in b) under stress will require a strain of ε_o against the stress because this is the strain associated with transforming between the variants. Therefore we can define a critical field at which the material should switch from one variant to another as $H_{crit} = (\sigma\varepsilon_o)/M_s$. One important addition to this argument must now be made. The relevant field for use in this equation is not the applied field, but the field inside the sample, the internal field. Therefore, we would expect to see a sudden strain occur in the material

when the internal field exceeds $(\sigma\varepsilon_o)/M_s$, the presence of demagnetization fields will likely shear over the ε vs. H_{appl} curve much like it shears an M vs. H loop in a magnetic material having surfaces normal to H. This demagnetizing effect will be accounted for here by subtracting the estimated demagnetization field from the applied field and comparing the strain response vs. internal field to model results.

Experimental evidence suggests that the concept of a critical internal field with a constant stress may be valid[5,6], but that the magnitude of this field is altered by the presence of hysteresis in the material. It is now proposed that the mechanism of hysteresis in FSMAs is associated with the phenomenon of yielding in the twinned martensite. The previous models assumed infinitely mobile twin boundaries, and hence zero mechanical yield stress. If we assume a perfectly plastic deformation, the model predicts the material will have a yield stress below which there is little deformation, and above which the material deforms continuously by twin boundary motion. This deformation model will now be added into the previous developments in modeling FSMA.

The yield stress gives rise to a mechanical energy in addition to that of the applied load that must be overcome by the magnetic field. Therefore, a sample that starts in a state such as that in Figure 1 a) will require a magnetic energy M_sH_{int} equal to the sum of the mechanical energies from the applied and yield stresses, $(\sigma_{app}+\sigma_y)\varepsilon_o$. Thus, the critical field upon application of magnetic field would be $H_{int}=((\sigma_{app}+\sigma_y)\varepsilon_o)/M_s$. This field is larger than that predicted by the model in the absence of yield stress. Once the sample has elongated, the critical stress at which the mechanical energy overcomes the magnetic energy is also changed by consideration of the yield stress. As the field is decreased, the applied mechanical energy must overcome the magnetic energy tending to keep the sample in its present state, as well as the yield energy that impedes motion of the twin boundaries regardless of direction. Therefore, the critical field upon ramping down the field will be $H_{int}=((\sigma_{app}-\sigma_y)\varepsilon_o)/M_s$. Figure 2 shows the predicted strain response with the consideration of hysteresis.

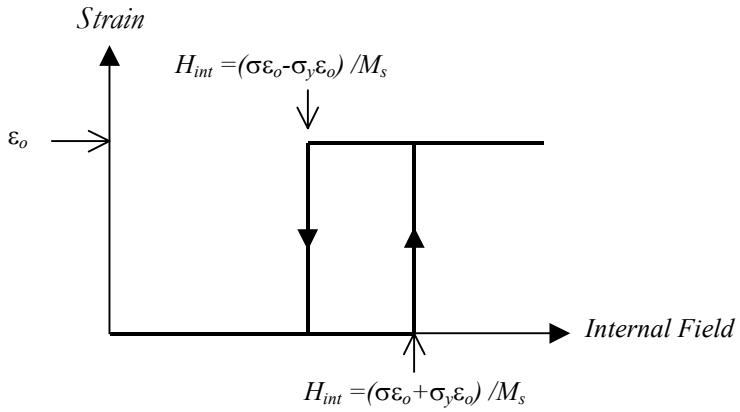

Figure 2. The predicted strain response of FSMA with a constant stress to internal field with the consideration of yield stress.

This concludes the development of the modeling to account for the cause of hysteresis in the material. This model is applied to a special case in this article, but can be expanded to a more general form based on the same principals.

3. EXPERIMENTAL

To test the models proposed, a special apparatus was constructed to measure strain under constant stress. This apparatus has been previously discussed in detail[5,6]. A mechanical testing machine was built around an adjustable-gap electromagnet with 100 mm diameter pole pieces capable of fields up to 800 kA/m. The load-bearing platens of the mechanical system are constructed of non-magnetic 303 stainless steel and aluminum. The vertically mounted aluminum cross-head slides on linear ball bearings from above the sample. An aluminum disk is affixed to the top of the cross-head to serve as a platform for loading. An eddy-current

proximity sensor affixed to this disk determines the vertical displacement of the cross head as the horizontal magnetic field is applied to the sample. The sensor is located far from the test region to isolate it from any fields from the electromagnet. This type of sensor is necessary because the large strains associated with the motions of twin boundaries in the sample make conventional strain gauges unsuitable. A Hall probe measures the applied magnetic field. As well as measuring deflection vs. applied field at constant load, this device is also used to measure deflection vs. load for loads added incrementally to the weight platform.

The samples tested were 14 mm by 6 mm by 6 mm prisms of $Ni_{49.8}Mn_{28.5}Ga_{21.7}$ single crystal grown by the Brigman technique. The boule was oriented by Laue back-reflection x-ray diffraction and cut by electric discharge machining (EDM) such that the martensitic *c*-axis could be aligned orthogonal to any of the walls of the sample by appropriate twin boundary motion. The sample composition was measured by electron probe micro-analysis.

In order to determine the demagnetizing field, a measurement of the sample's magnetization behavior was necessary. It is important to make a distinction between the magnetization processes caused by twin motion, and that caused by rotation of the magnetization within the unit cell. Therefore, a constrained sample technique was devised to test the magnetic properties of the material without the possibility of twin motion. A thin square sample was cut from a single crystal boule with sides corresponding to planes normal to the directions that could be magnetic easy axes. The sample was biased into a single variant state by the application of a magnetic field of 800 kA/m before potting. In order to allow the magnetization to rotate away from its easy axis without the possibility of twin motion, the sample was constrained by potting it inside Struers brand mounting epoxy. Thus this sample could be magnetized by magnetization rotation without any twin motion. This hard clear epoxy was poured over the sample in a mold to form a solid disk of epoxy with the sample inside. This sample was then tested in a vibrating sample magnetometer for magnetization response versus applied field. This data can then be used in determining the magnetization state of the material before any strain is evident.

4. RESULTS

Measurements of mechanical, magnetic, and magneto-mechanical properties were taken. Mechanical and magnetic measurements were made to determine yield stress and permeability for use in the model described in Section 2, and the magneto-mechanical measurements provide the data to compare with the model predictions. The results of mechanical testing of stress vs. strain are shown in Figure 3. The yield stress for this crystal is approximately 0.8 MPa. It is evident that the material is not perfectly plastic, as the stress needed to cause deformation after yielding does increase by about 1 MPa over a range of 6% strain. This increase in stress must be overcome when driving the material.

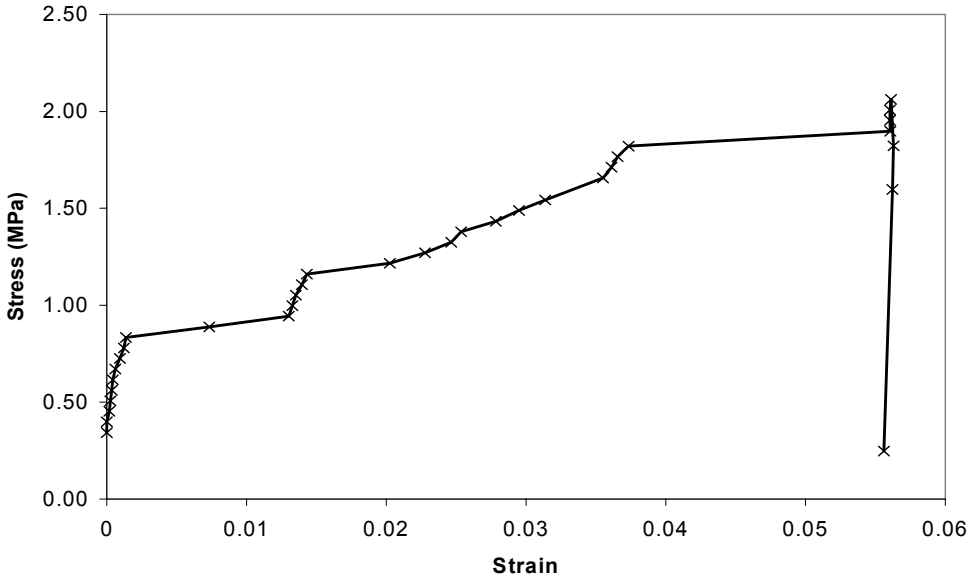

Figure 3. Mechanical characterization of a martensitic Ni-Mn-Ga single crystal.

The results of the vibrating sample magnetometer measurement of magnetization, *M* vs. field, *H* are shown for two directions of applied field in Figure 4. The easy direction, shown in gray is the direction in which the *c*-axis was biased previous to potting the sample. The hard direction, shown in black is orthogonal to the easy direction. Magnetization in the hard direction is of interest because it will characterize the rotation of the magnetization away from the easy crystal direction without the motion of a twin boundary. This rotation occurs with a relative permeability of about 2.1. This figure will be useful in distinguishing between the applied field and the internal field which actually drives twin boundary motion.

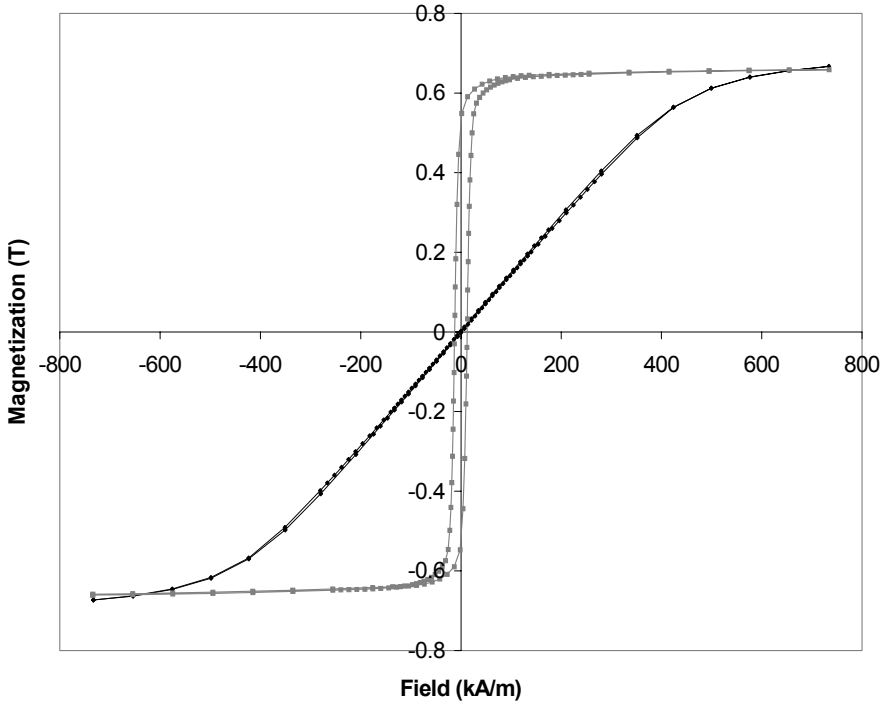

Figure 4. VSM measurement of magnetization versus applied field in the easy (gray) and hard (black) directions in a constrained single crystal. The easy direction corresponds to magnetization along the *c*-axis in the sample.

The results of magneto-mechanical characterization are seen in Figure 5 and Figure 6. Figure 5 illustrates the strain in a sample vs. applied field at a variety of constant strains. This figure is different than the prediction of Figure 2 in that the strain is plotted vs. applied field rather than internal field. Some of the measured curves will be corrected for internal field in the next section and compared to predictions. The blocking stress for the sample appears to be about 2 MPa, at which point the strain response drops off rapidly. It should also be noted that for most applied stresses, the full width of the hysteresis is about 250 kA/m ($H_c \approx$ 125kA/m). This hysteresis increases dramatically as the strain response falls off near the blocking stress.

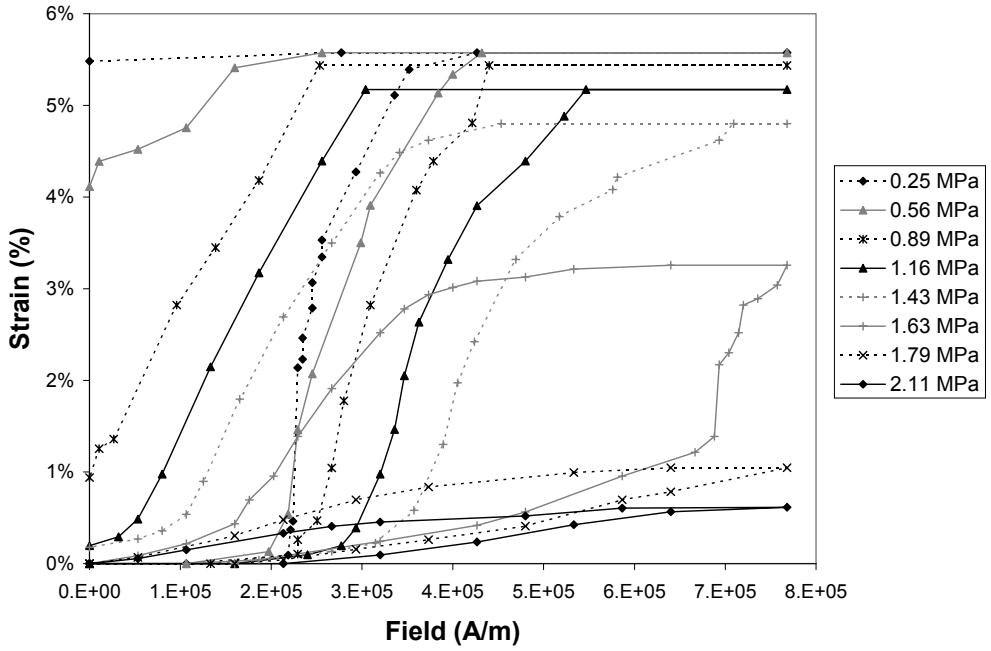

Figure 5. Magneto-mechanical response of Ni-Mn-Ga at various constant stress levels.

Figure 6 depicts the surface structure of the crystal as twin boundary motion is taking place. The diagonal bands come from surface ridging over individual variants separated by twin boundaries. The variants with their *c*-axis in the direction of the load are seen slightly darker than the variants with their *c*-axis in the direction of the field. As the field is ramped up, the variants favored by the field begin to grow, and eventually transform the entire crystal to a variant favored by the field. The sample was approximately 14 mm long, and elongated by about 0.8 mm under application of the field.

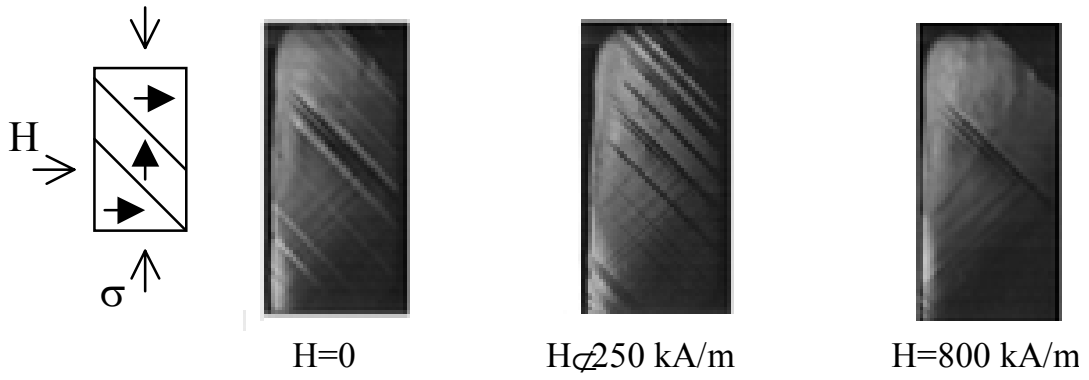

Figure 6. Photographs of the Ni-Mn-Ga single crystal during actuation. The far left figure shows the condition of the sample with zero applied field. As the field increases to 800 kA/m in the far right photograph, the field-favored (c-axis horizontal) grow at the expense of the load-favored variants.

5. DISCUSSION

The data for mechanical and magneto-mechanical response will now be used to compare the theoretical predictions of Section 2 to laboratory data. The most difficult step in linking the two is the estimation of the internal field, which allows us to account for demagnetization effects. The first step in estimating the internal field is to assume that we can apply the relation $H_{int} = H_{appl} - NM$, and estimate a value for N, the demagnetization factor. The value NM is also called the demagnetization field H_d. N is only a constant for ellipsoids of revolution, but for simplicity we will assume a constant value for our prismatic samples. The only alternative would be to use finite-element solutions. The samples tested were magnetized laterally, and had aspect ratios of about 2.3. To estimate the lateral demagnetization factor, we can start by noting that N along the length of a rod with aspect ratio 2 is 0.14. As well, for three orthogonal directions, $N_x + N_y + N_z = 1$. In our samples, N_z would be close to the 0.14 figure for the rod, and $N_x = N_y$ from symmetry, giving us an estimate for transverse N of about 0.4. Field-induced twin boundary motion rotates the magnetization from an axial to a transverse direction. This process requires a magnetostatic energy of $\frac{1}{2}\Delta N M_s^2$ where ΔN is $N_{perp} - N_{parallel}$. We now must determine the magnetization behavior of the sample to find the demagnetization field. This estimation involves many assumptions and is likely a primary source of error. When the sample is fully magnetized, the saturation magnetization is about 0.65T, thus H_d will be equal to about 155 kA/m. This field is significant compared to the applied fields. To a first approximation it shears the vertical loops of the model so that the saturation field occurs at an applied field greater by 155kA/m than the field at which twin motion begins. Modeling the magnetization in the sample allows us to plot the results of strain vs. internal field at constant load as seen for two values of stress in Figure 7..

The model predictions of coercivity in Fig. 7 agree with the data adjusted to the internal field scale and the shape of the curves is close to that predicted, but not as square. Two major sources of error likely account for the discrepancy. As discussed in the previous paragraph, many assumptions were made in estimating the internal field. The assumption of a uniform internal field is certainly not correct, but provided a good place to start the analysis. As well, the magnetization state of the material was estimated from previous measurements of magnetization with field and the known strain state. A direct measurement of magnetization as the sample is straining would provide the most accurate characterization of the material. The other source of error is the assumption of perfectly plastic mechanical behavior. Figure 3 shows that this is not strictly the case, but that the internal resistance to deformation increases with strain. This could cause the internal field necessary to cause strain to increase with strain as is seen in Figure 7.

Even with these sources of error present, the data is close to the forms of the predicted curves in both shape and magnitude, so it is likely that the fundamental ideas concerning the relationship between internal field, external stress, and yield stress are correct. Further precision could be gained by measurement of the magnetization *in-situ* while a sample is undergoing field-induced strain. This would allow for the most accurate estimation of the internal field. As well, more accurate modeling of the mechanical behavior may improve the predictions of the model while adding complexity.

The important result here is the relevance of the yield stress to the hysteresis of the material. This hysteresis will govern the useful work that the material can perform against a load in a repeatable fashion. A present, most of the energy input to the material is consumed in the hysteresis. By decreasing the yield stress, this hysteresis should also decrease providing more useful material for engineering applications.

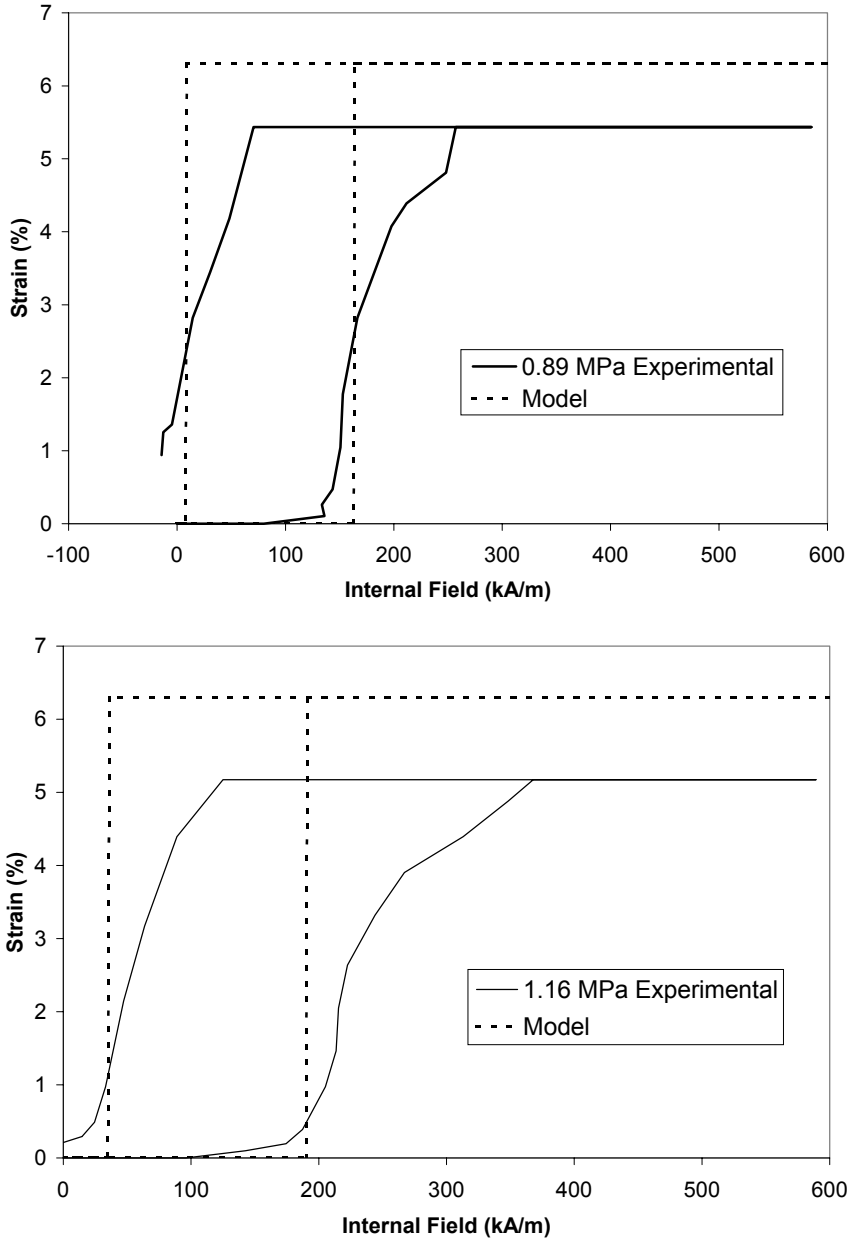

Figure 7. Comparison of collected data for strain versus estimated internal field and modeling for two values of constant stress.

ACKNOWLEDGEMENTS

This work was supported by a subcontract from Boeing on a DARPA contract, by the Finnish Academy of Sciences (TEKES) through the Helsinki University of Technology and by grants from ONR and DARPA. The high speed video images were taken by Miguel Marioni.

REFERENCES

1. K. Ullakko, J.K. Huang, C. Kantner, V.V. Kokorin and R.C. O'Handley, "Large magnetic field- induced strains in Ni2MnGa single crystals," *Appl. Phys. Lett.,* **69**, 1966 (1996).

2. R.D. James and M. Wuttig, "Magnetostriction of Martensite", *Phil. Mag A* **77**, 1273 (1998).

3. R. Tickle, R. D. James, T. Shield, M. Wuttig, and V.V. Kokorin, "Ferromagnetic shape memory in the NiMnGa system," *IEEE Trans. Magn*. **35**, 4301 (1999).

4. R. C. O'Handley, "Model for Strain and Magnetization on Magnetic Shape Memory Alloys" *J. of Appl. Phys.* **83**, 3262-3270 (1998).

5. S. J. Murray, R.C. O'Handley, and S. M. Allen, "Model for Discontinuous Actuation of Ferromagnetic Shape Memory Alloy under Stress" *J. Appl. Phys*., in press.

6. S. J. Murray, R. C. O'Handley and S.M. Allen, "Modeling and Experiments for Deformation under Load in Ni-Mn-Ga Ferromagnetic Shape Memory Alloy," *Proceedings of the MRS*, In Press.